Electronic Supplementary Material (ESI) for Journal of Materials Chemistry A.

Supplementary information

Adjusting the optical band gap of $CsPbBr_{3-y}X_y$ (X = Cl, I) for optimal interfacial charge transfer and enhanced photocatalytic hydrogen generation

Marija Knezevic,[1] Vien-Duong Quach,[1] Isabelle Lampre,[1] Marie Erard,[1] Pascal Pernot,[1] David Berardan,[2] Christophe Colbeau-Justin,[1] Mohamed Nawfal Ghazzal[1]

[1]*Institut de Chimie Physique, UMR 8000 CNRS, Université Paris-Saclay, F-91405 Orsay*
[2]*Institut de Chimie Moléculaire et des Matériaux d'Orsay, UMR 8182 CNRS, Université Paris-Saclay, F-91405, Orsay*
mohamed-nawfal.ghazzal@universite-paris-saclay.fr

Materials

All chemicals were used without further purification. Cesium carbonate ($CsCO_3$, Acros Organics, 99.5 %), lead bromide ($PbBr_2$, Acros Organics, 99%), oleic acid (OA, Riedel de Haën), 1-octadecene (ODE, Sigma Aldrich, 90 %), oleylamine (OAm, Acros Organics, 80-90 %), toluene (Sigma Aldrich, 99.8 %), n-hexane (Sigma Aldrich, 95 %), lead chloride ($PbCl_2$, Acros Organics, 99%), trioctylphosphine (Sigma Aldrich, 97 %), lead iodide (Acros Organics, 99 %), HCl (Sigma Aldrich, ACS reagent, 37 %), titanium(IV) isopropoxide (TTiP, Sigma Aldrich, 97 %), titanium diisopropoxide bis (acetylacetonate) (TAA, Sigma Aldrich, ≥ 75 % in isopropanol), titanium(IV) butoxide (TBOT, Sigma Aldrich, 97 %), titanium(IV) chloride ($TiCl_4$, Sigma Aldrich, for synthesis), tetrabutylammonium hexafluorophosphate ($(Bu_4N)(PF_6)$, Sigma Aldrich, ≥ 98 %), dichloromethane (DCM, Sigma Aldrich, ≥ 99.8 %), acetonitrile (CH_3CN, Sigma Aldrich, ≥ 99.9 % for HPLC).

Table S1. Bandgap-estimation using Kubelka-Munk modified function

	Eg^{opt} (eV)
$CsPbCl_3$	2.95
$CsPbBr_{1.65}Cl_{1.35}$	2.60
$CsPbBr_{1.95}Cl_{1.05}$	2.51
$CsPbBr_3$	2.34
$CsPbBr_{1.95}I_{1.05}$	2.14
$CsPbBr_{1.65}I_{1.35}$	2.06

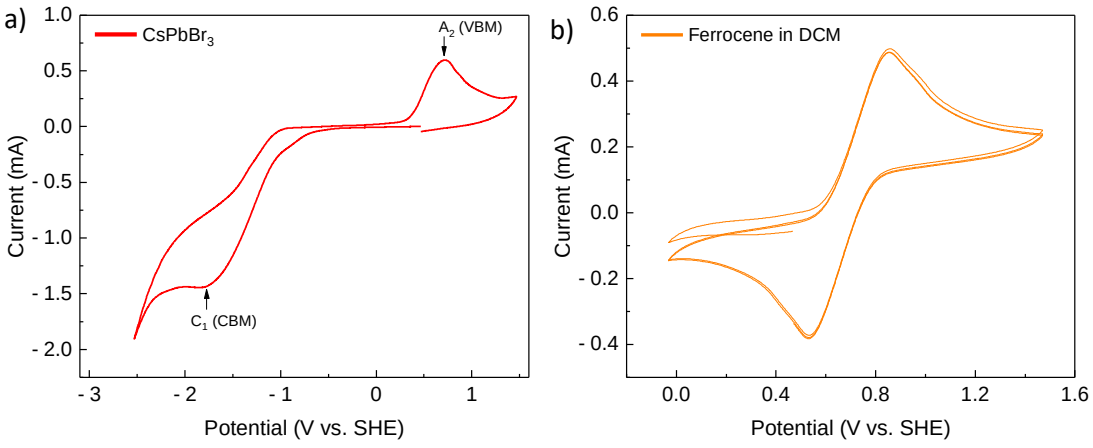

Figure S1. Cyclic voltammogram of $CsPbBr_3$ nanocrystals, recorded at 50 $mV.s^{-1}$ in a solution of 100 mM $(Bu_4N)(PF_6)$ in DCM. (b) Three-scanned cyclic voltammogram of Fc/Fc^+ redox couple. Conditions: TBAHFP 0.1M in DCM as a supporting electrolyte, scan rate 50 $mV.s^{-1}$

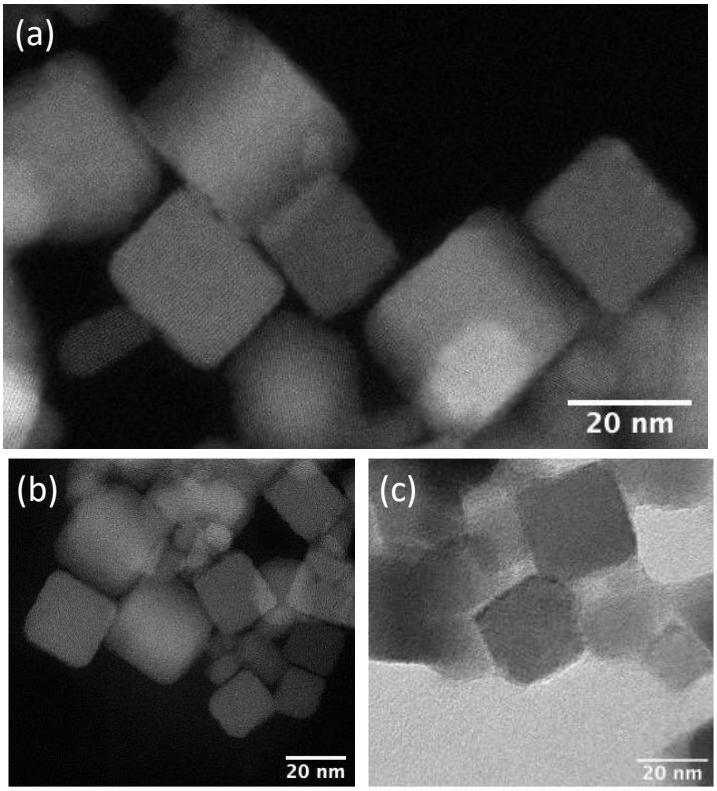

Figure S2. (a,b) STEM and (c) TEM images of $CsPbBr_3$

Tetragonal $CsPbCl_3$ and non-perovskite orthorhombic $CsPbI_3$ NCs nanoparticles were synthesized by a hot injection colloidal synthesis method.[1,2] Degradation from the dark red to the yellow non-perovskite $CsPbI_3$ was observed quickly after drying since it is a thermodynamically favored phase at ambient conditions,[3] whereas $CsPbCl_3$ remains tetragonal below 47 °C. However, $CsPbCl_3$ is not a single-phase perovskite, there is an unidentified peak at ~2θ=52°.5).[4]

Table S2. Lattice parameters, space group, and crystal symmetry of $CsPbX_3$, (X = Cl, Br, I)

	Lattice parameters (Å)			Space group	Crystal symmetry
	a	b	c		
$CsPbCl_3$	5.584	5.584	5.617	P4/mbm	tetragonal perovskite
$CsPbBr_{1.65}Cl_{1.35}$	8.218	11.444	8.123	Pnma	
$CsPbBr_{1.95}Cl_{1.05}$	8.256	11.495	8.167	Pnma	
$CsPbBr_3$	8.257	11.753	8.210	Pnma	orthorhombic perovskite
$CsPbBr_{1.95}I_{1.05}$	8.351	11.925	8.329	Pnma	
$CsPbBr_{1.65}I_{1.35}$	8.413	11.997	8.368	Pnma	
$CsPbI_3$	4.810	10.465	17.783	Pmnb	non-perovskite orthorhombic

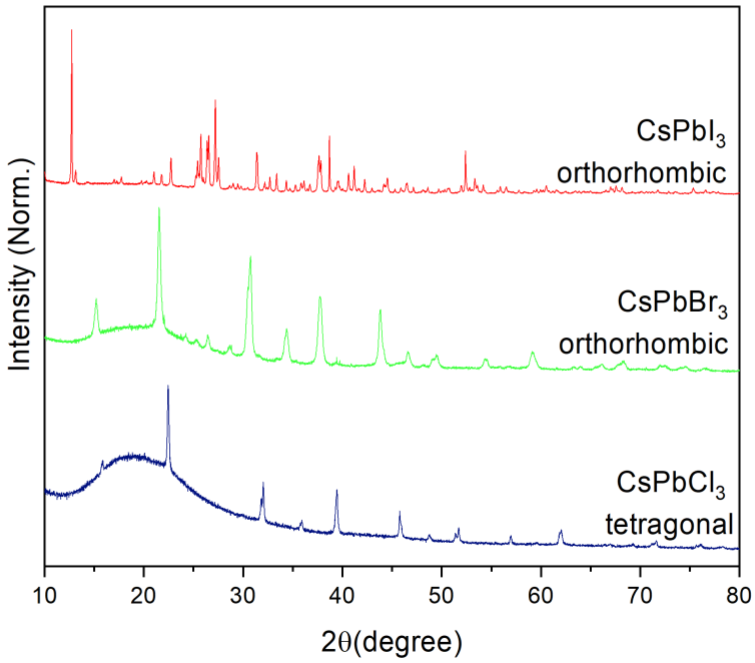

Figure S3. XRD patterns of $CsPbBr_3$, $CsPbCl_3$, and $CsPbI_3$.

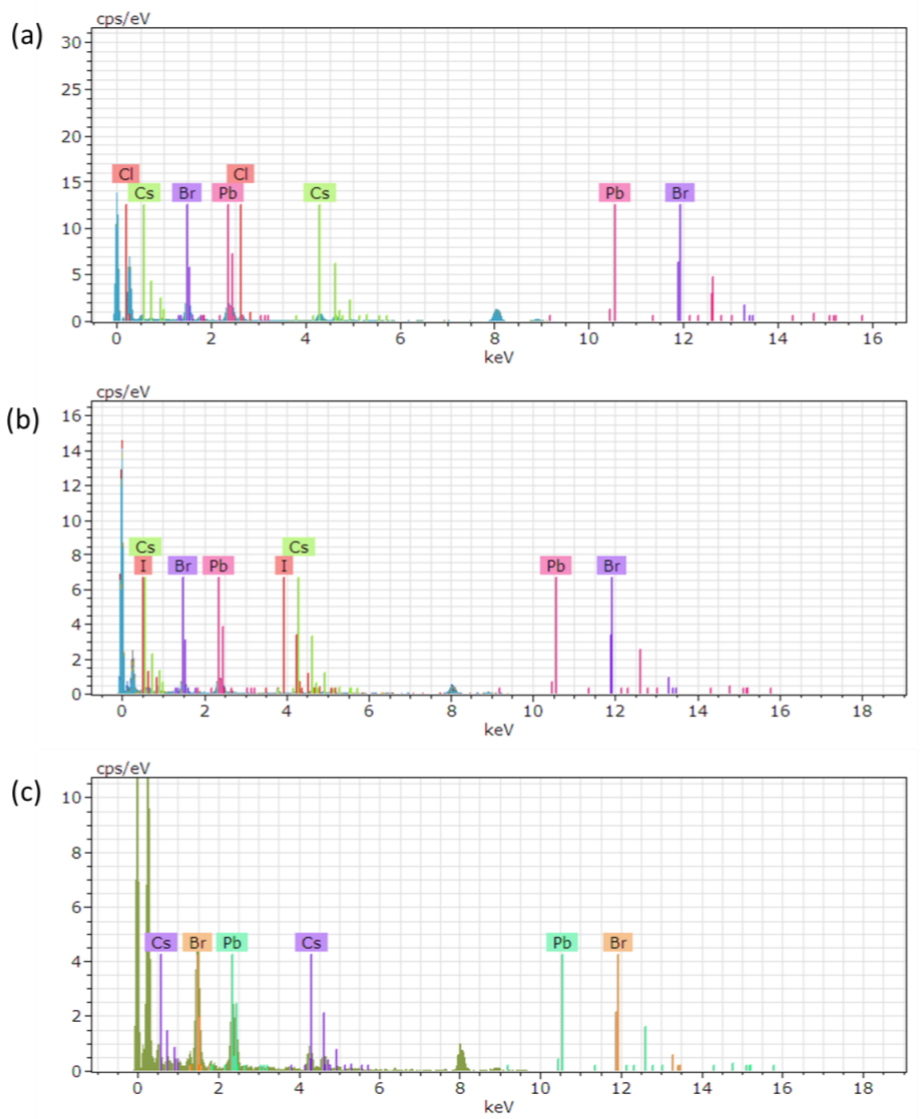

Figure S4. EDS spectra of (a) $CsPbBr_{1.95}Cl_{1.05}$, (b) $CsPbBr_{1.95}I_{1.05}$, and (c) $CsPbBr_3$.

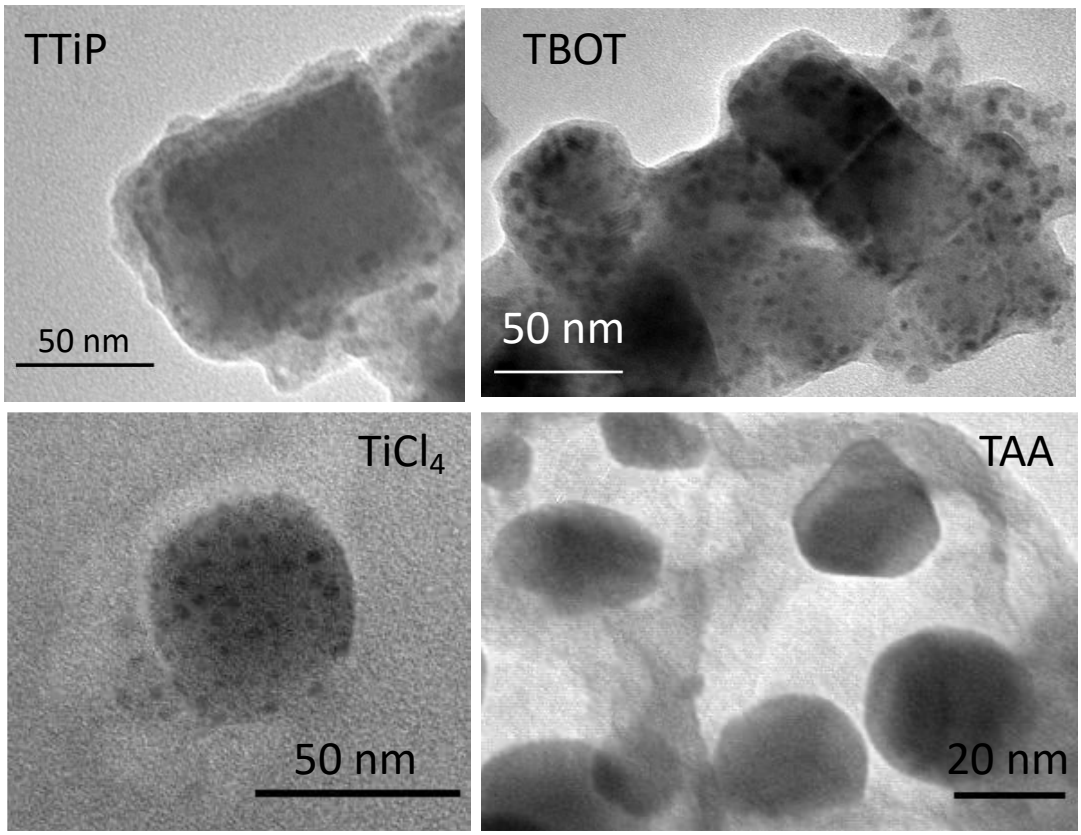

Figure S5. TEM images of $CsPbBr_3$ coated with TTiP, TBOT, $TiCl_4$, and TAA.

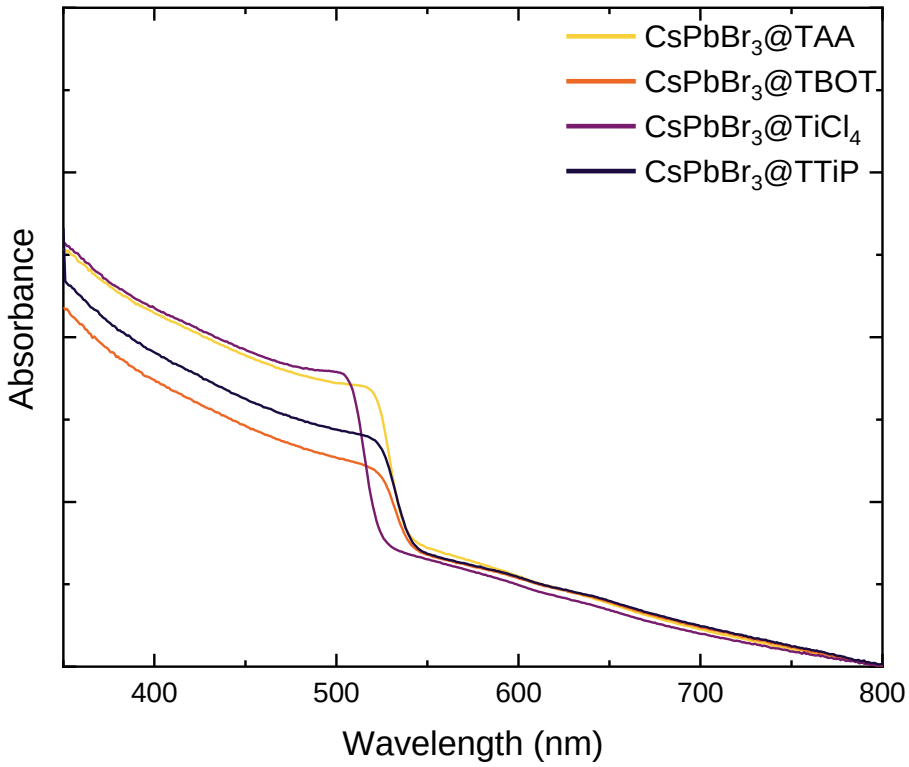

Figure S6. DRS spectra of $CsPbBr_3$ coated with different TiO_2 precursors: TAA, TBOT, TTiP, and $TiCl_4$.

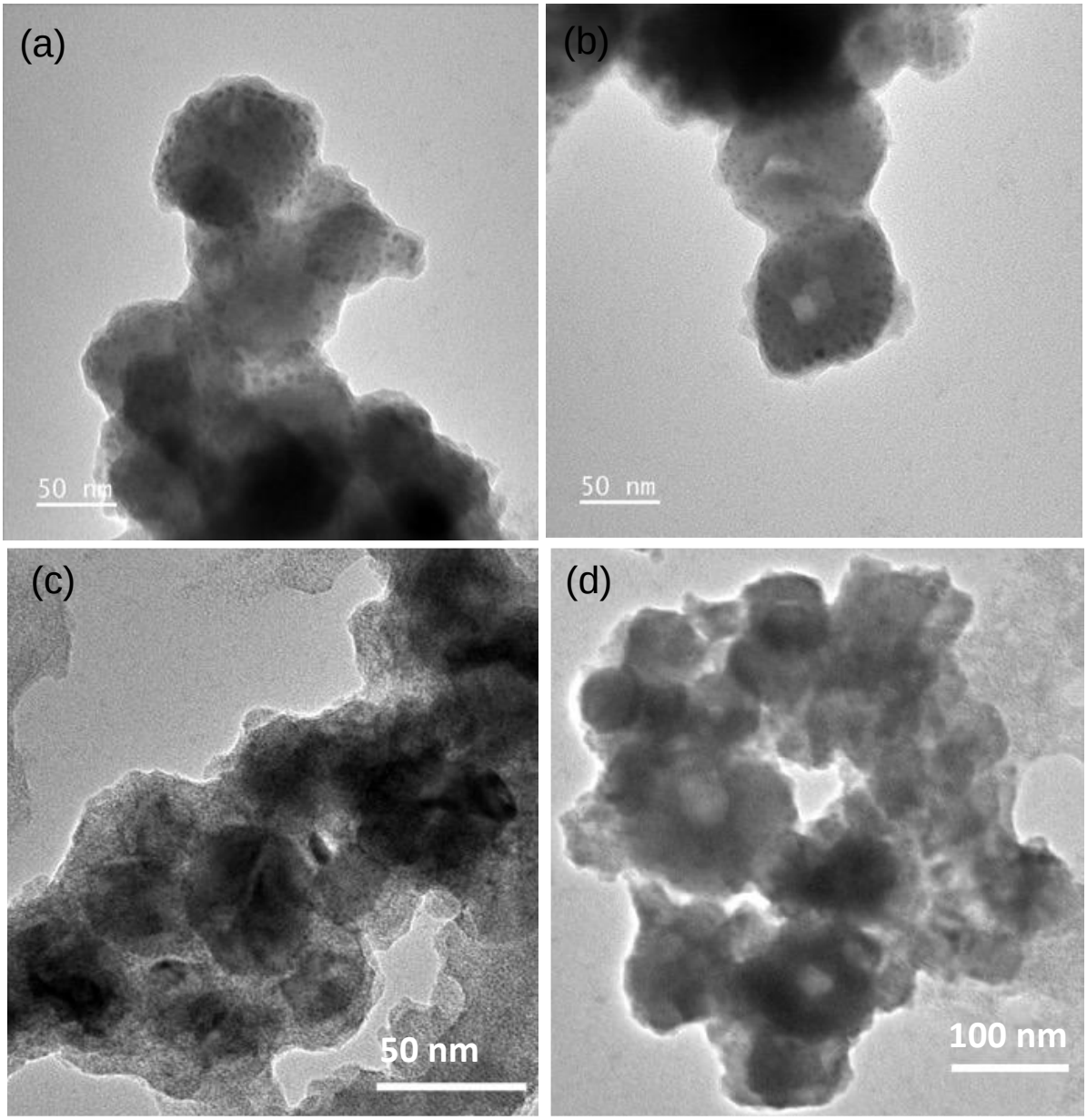

Figure S7. TEM images of $CsPbBr_3$ covered by TiO_x overlayer ($CsPbBr_3$@TiO_x).

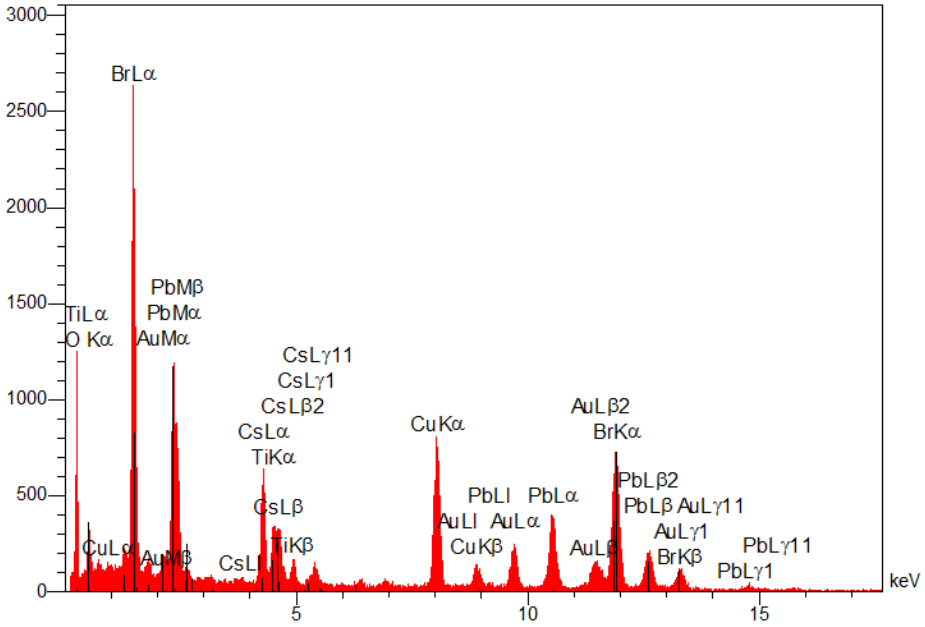

Figure 8. EDS spectra of $CsPbBr_3$@TiO_2

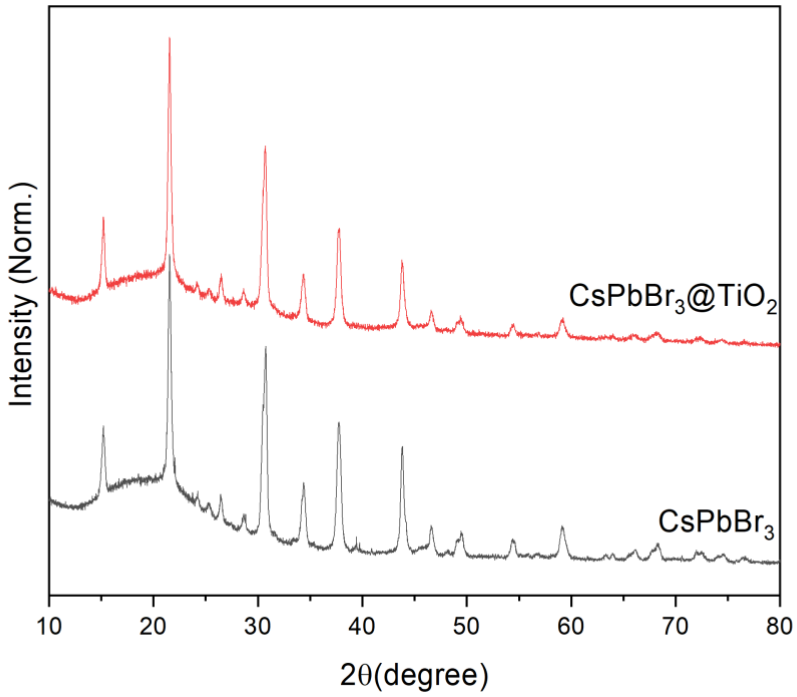

Figure S9. XRD patterns of $CsPbBr_3$ and $CsPbBr_3$@TiO_2 upon calcination at 300 °C under ambient conditions.

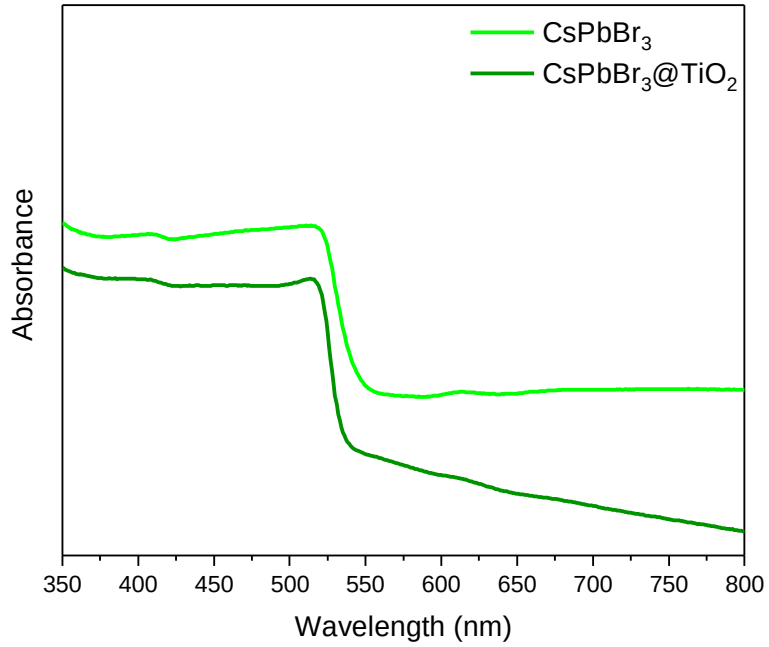

Figure S10. DRS spectra of $CsPbBr_3$ and $CsPbBr_3@TiO_2$ upon calcination at 300 °C under air.

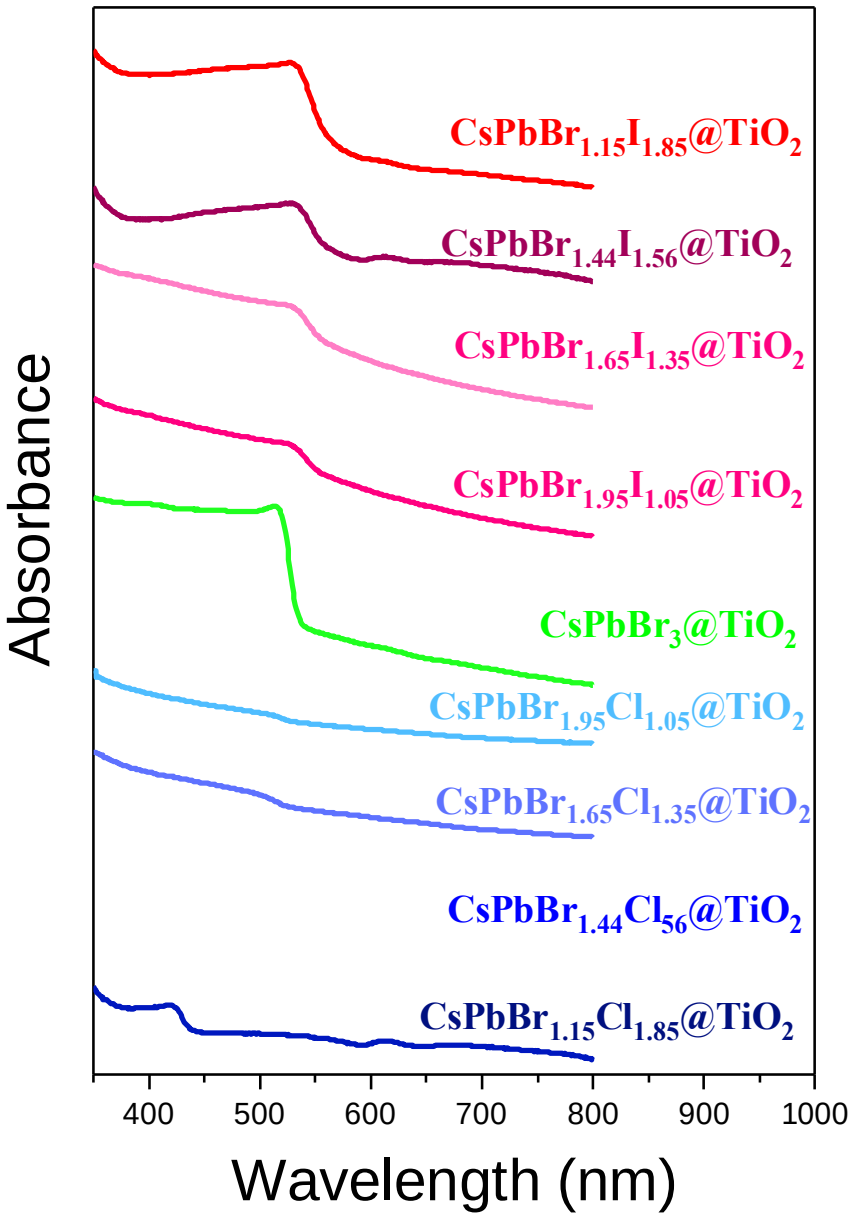

Figure S11. DRS spectra of anion-substituted $CsPbBr_3@TiO_2$ with variable amounts of PbI_2 and $PbCl_2$

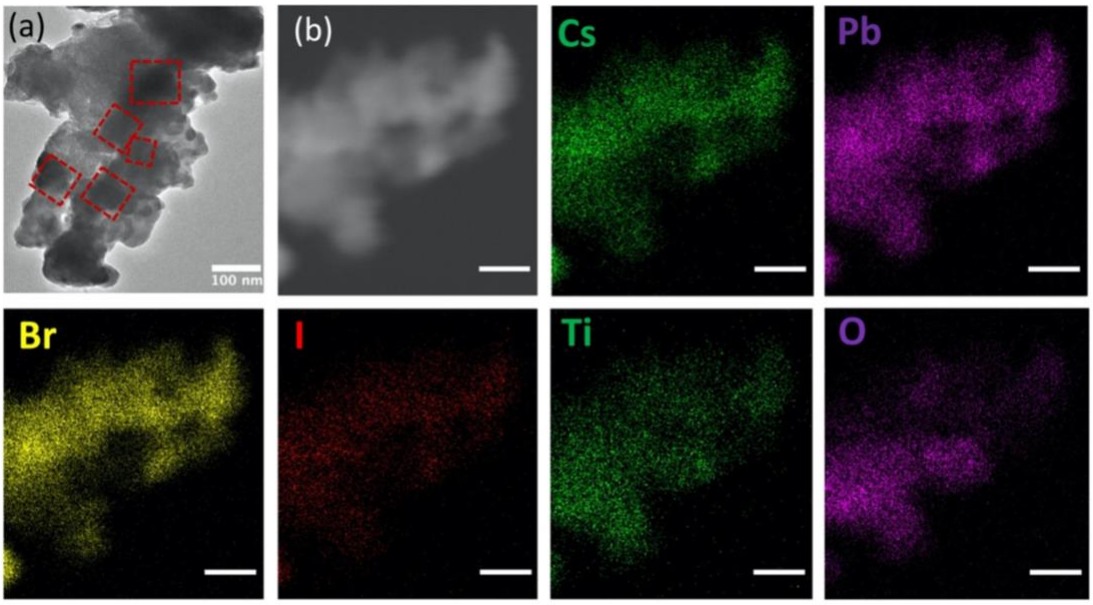

Figure S12. (a) TEM image and (b) STEM-EDS mapping of $CsPbBr_{1.95}I_{1.05}@TiO_2$. The scale bar corresponds to 100 nm.

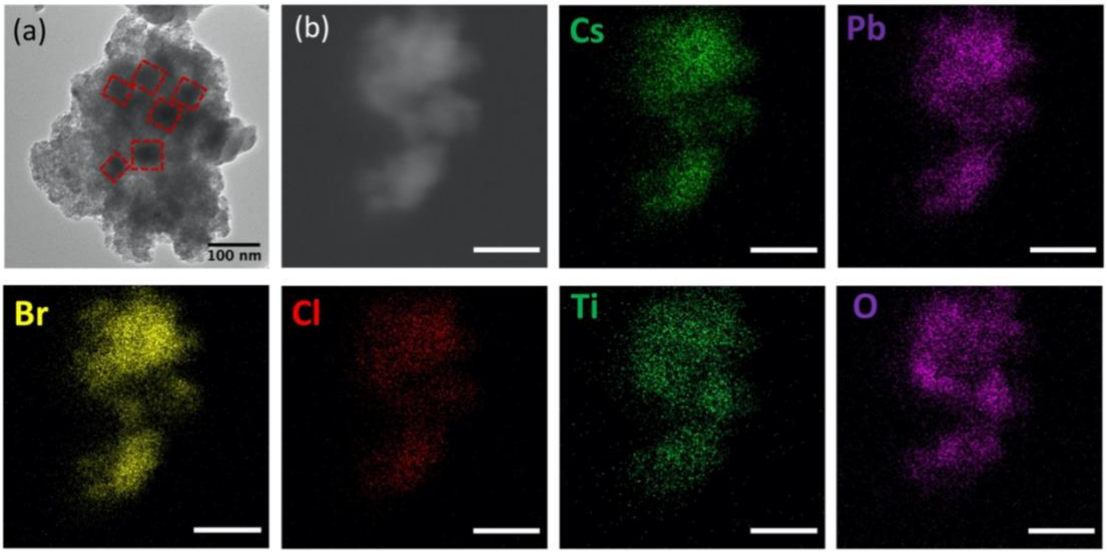

Figure S13. (a) TEM image and (b) STEM-EDS mapping of $CsPbBr_{1.95}Cl_{1.05}@TiO_2$. The scale bar corresponds to 100 nm.

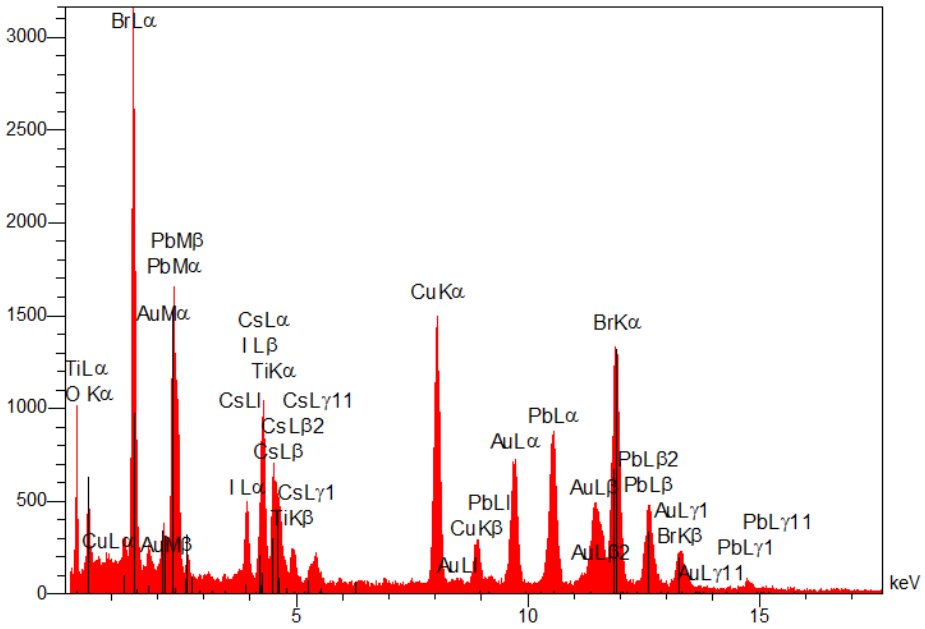

Figure 14. EDS spectra of $CsPbBr_{1.95}I_{1.05}$ @TiO_2

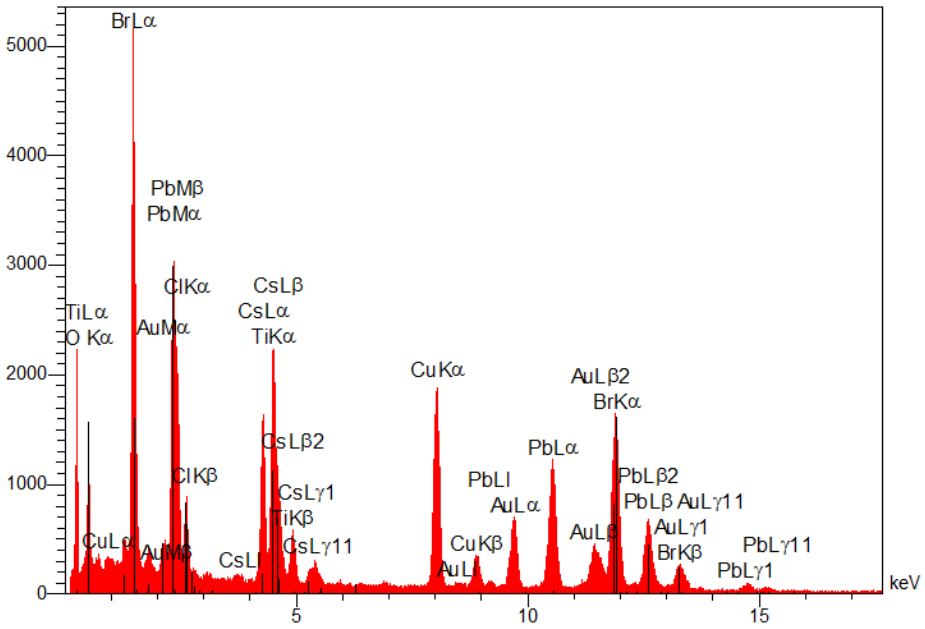

Figure S15. EDS spectra of $CsPbBr_{1.95}Cl_{1.05}$ @TiO_2

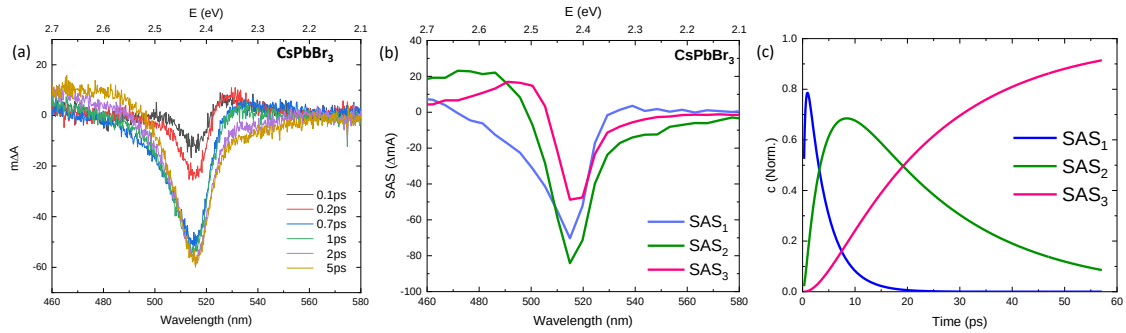

Figure S16. (a) TA spectra of $CsPbBr_3$ excited at 390 nm with a fluence of 418 μj cm^{-1}, (b) species-associated spectra (SAS), and (c) their temporal evolution obtained from global target analysis for $CsPbBr_3$.

Table S3. Time-decay constants of $CsPbBr_{3-y}X_y$ (X = Cl, I) obtained with a global target analysis using a sequential model, for the spectro-kinetics data recorded at 390 nm excitation with a fluence of 418 μJ cm^{-2}

	t_0 (ps)	t_1(ps)	t_2 (ps)
$CsPbBr_{1.65}Cl_{1.35}$	0.2	5.9	25
$CsPbBr_{1.95}Cl_{1.05}$	0.2	3.0	25
$CsPbBr_3$	0.3	3.3	27
$CsPbBr_{1.95}I_{1.05}$	0.3	5.3	17
$CsPbBr_{1.65}I_{1.35}$	0.5	5.6	12

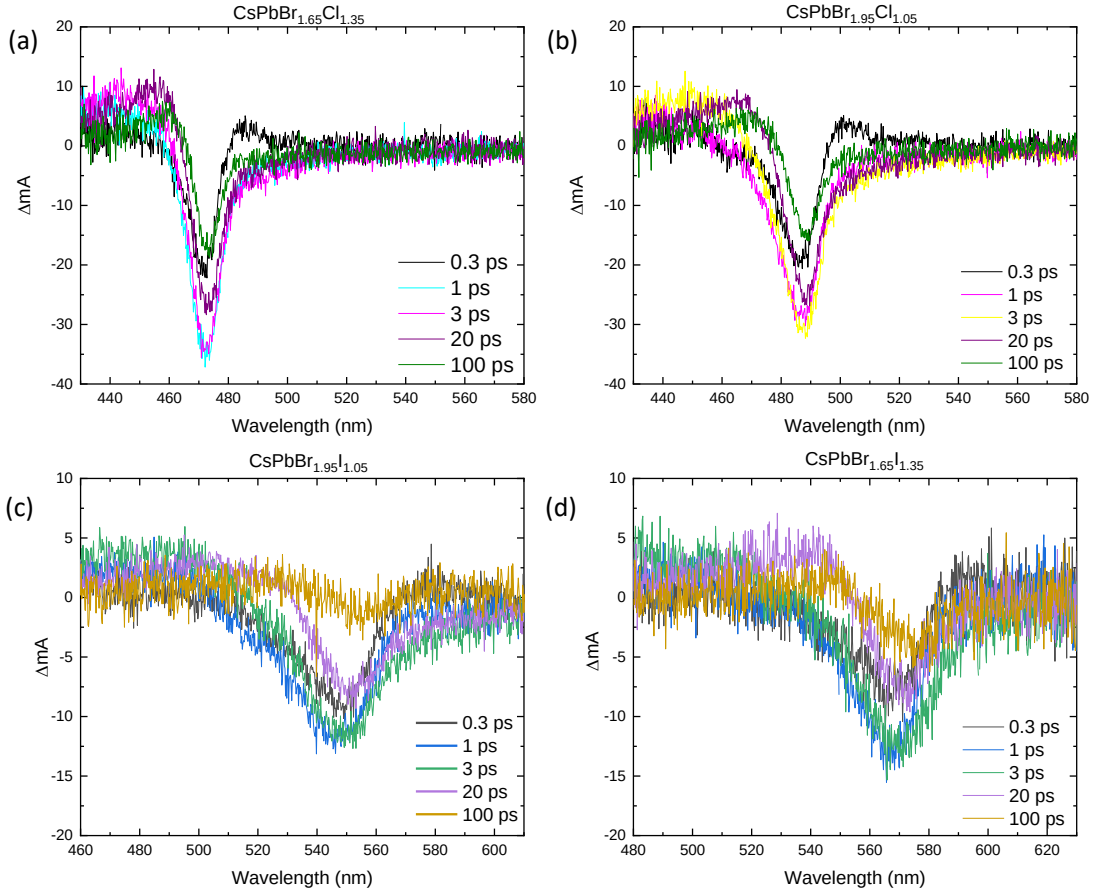

Figure S17. TA spectra of $CsPbBr_{3-y}X_y$ (X = Cl, I) excited at 390 nm with a fluence of 418 μJ cm^{-2}

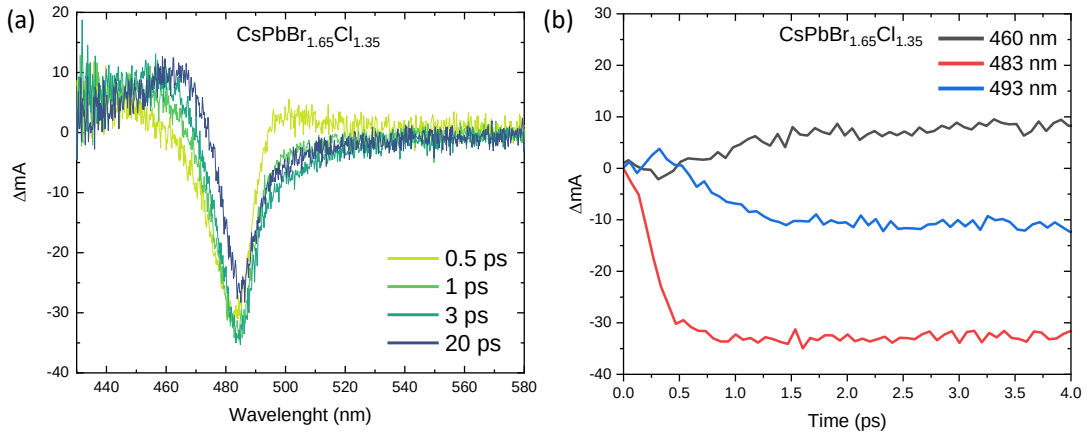

Figure S18. (a) TA spectra and (b) kinetics traces of $CsPbBr_{1.65}Cl_{1.35}$ excited at 390 nm, at an excitation density of 209 μJ cm^{-2}

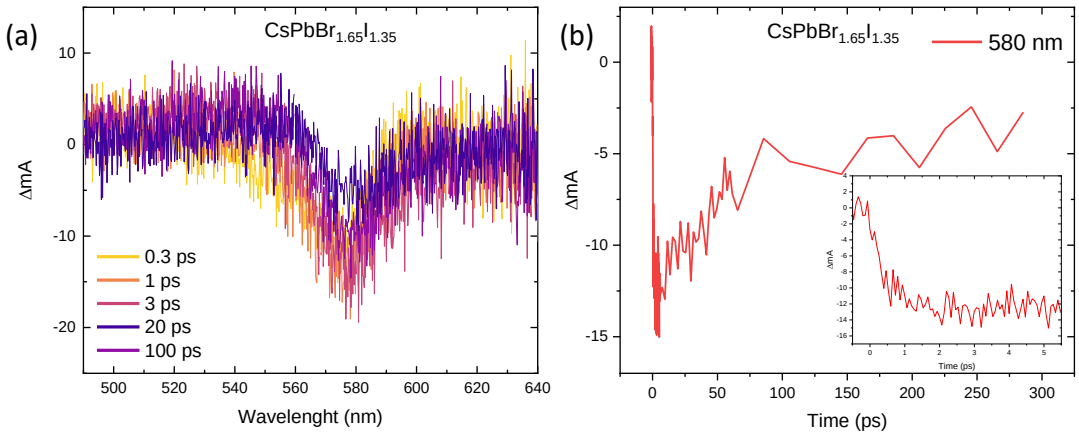

Figure S19. (a) TA spectra and (b) kinetics traces of $CsPbBr_{1.65}I_{1.35}$ excited at 390 nm with a fluence of 209 μJ cm^{-2}

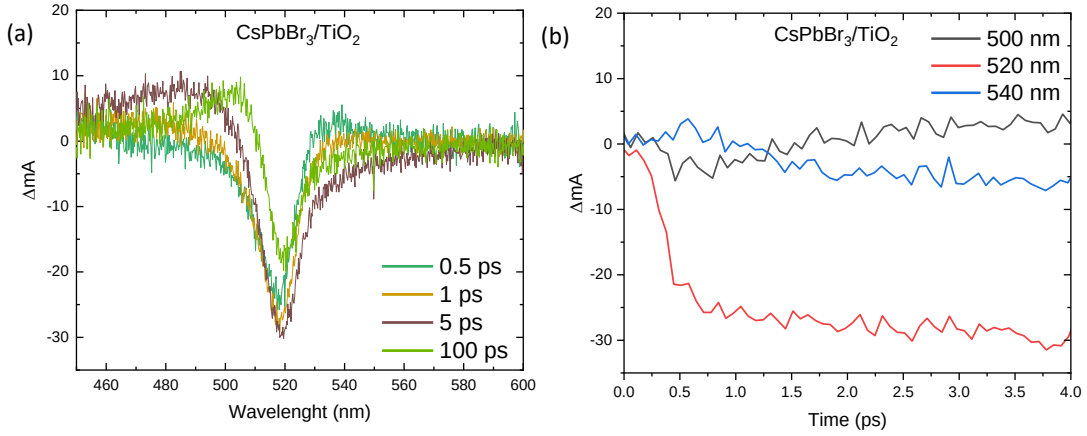

Figure S20. (a) TA spectra and kinetics traces of $CsPbBr_3$ and (b) $CsPbBr_3/TiO_2$ excited at 390 nm with a fluence of 209 μJ cm^{-2}

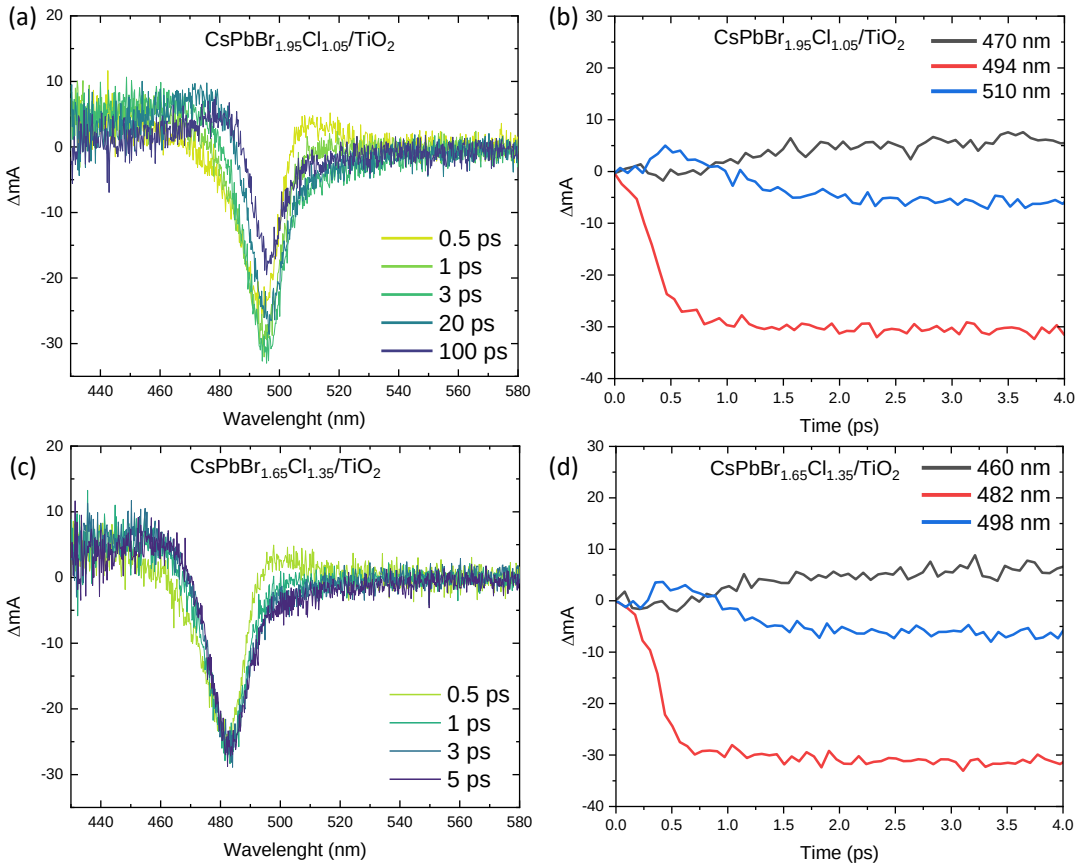

Figure S21. (a,b) TA spectra and kinetics traces of $CsPbBr_{1.95}Cl_{1.05}/TiO_2$ and (c,d) $CsPbBr_{1.65}Cl_{1.35}/TiO_2$ excited at 390 nm with a fluence of 209 μJ cm^{-2}

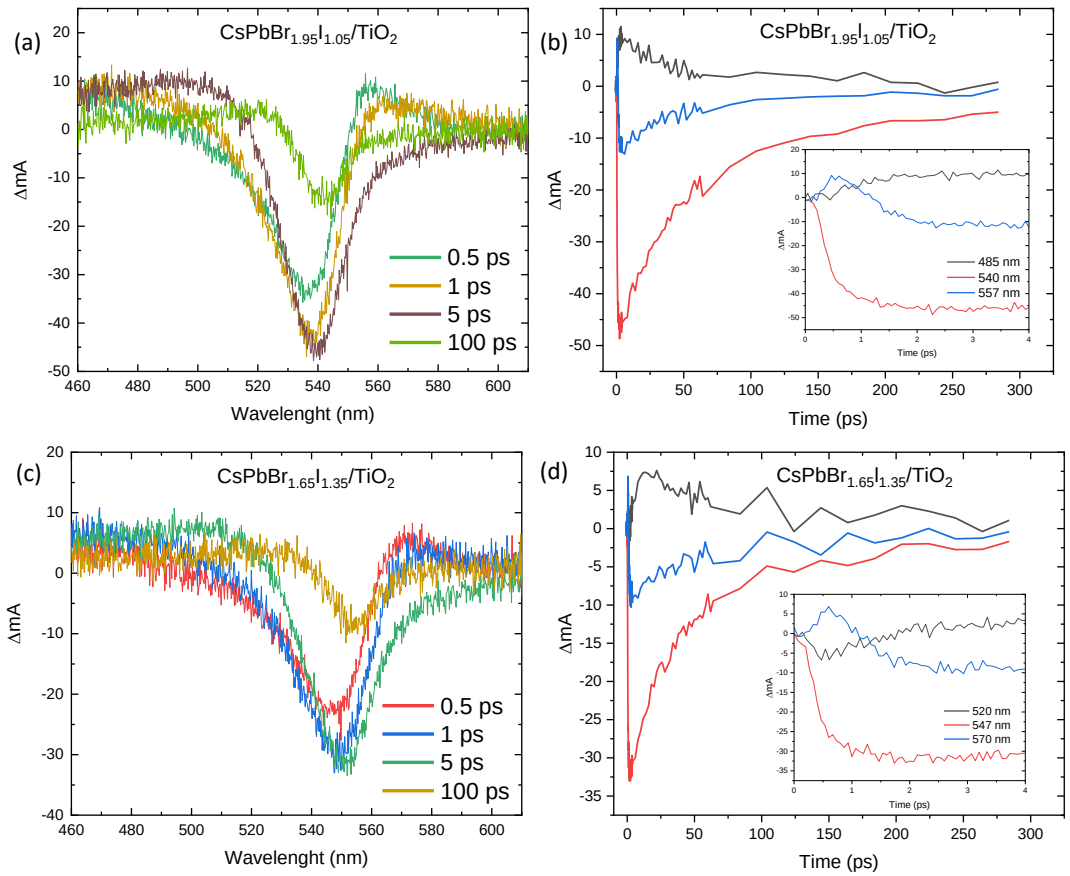

Figure S22. (a,b) TA spectra and kinetics traces of $CsPbBr_{1.95}I_{1.05}/TiO_2$ and (c,d) $CsPbBr_{1.65}I_{1.35}/TiO_2$ excited at 390 nm with a fluence of 209 μJ cm^{-2}

Table S4. Photoluminescence lifetimes of $CsPbBr_{3-y}X_y$ (X = Cl, I)

	t_1 (ns)	t_2 (ns)	t_3 (ns)	t_4 (ns)	t_{av}
$CsPbBr_{1.65}Cl_{1.35}$	11±0.26	2.13±0.04	0.52±0.02	0.11±0.01	1.53±0.03
$CsPbBr_{1.95}Cl_{1.05}$	13±0.13	2.49±0.02	0.58±0.01	0.10±0.01	3.28±0.03
$CsPbBr_3$	8.9±0.17	1.33±0.04	0.22±0.01	-	2.42±0.04
$CsPbBr_{1.95}I_{1.05}$	5.2±0.15	1.23±0.03	0.41±0.013	0.12±0.01	0.39±0.01
$CsPbBr_{1.65}I_{1.35}$	5.8±0.24	1.49±0.06	0.58±0.02	0.25±0.01	0.58±0.01

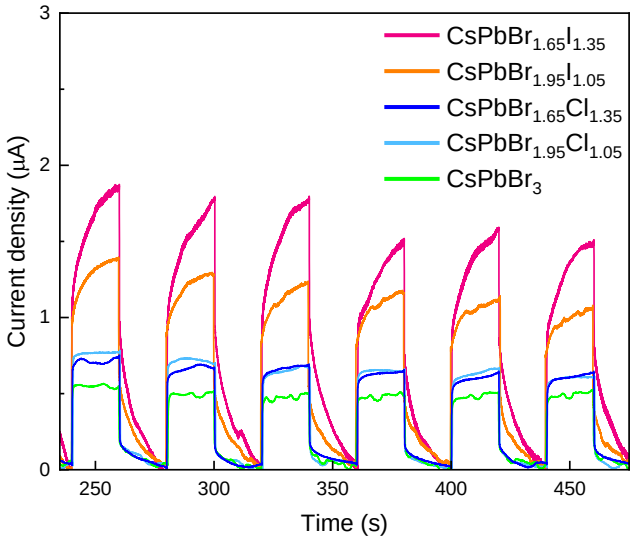

Figure S23. Amperometric I-t curves at a bias potential of 0.7 V vs Ag/Ag^{+} under simulated solar light irradiation with 20 s light on/off cycles of MHPs

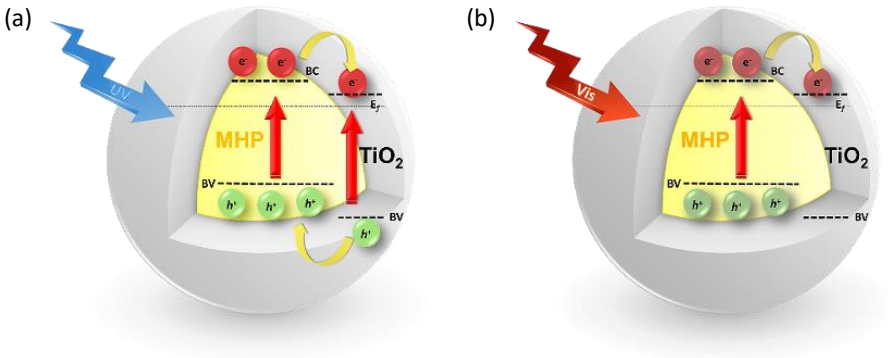

Figure S24. Schematic representation of electron transfer mechanism in $CsPbBr_{3-y}X_y$ (X = Cl, I) core@shell nanostructure under (a) UV and (b) visible excitation.

Table S5. Photoluminescence lifetimes of $CsPbBr_{3-y}X_y@TiO_2$ (X = Cl, I)

	t_1 (ns)	t_2 (ns)	t_3 (ns)	t_4 (ns)	t_{av} (ns)
$CsPbBr_{1.65}Cl_{1.35}@TiO_2$	6.48±0.09	1.64±0.04	0.39±0.01	0.081±0.001	0.38±0.004
$CsPbBr_{1.95}Cl_{1.05}@TiO_2$	5.70±0.15	1.39±0.04	0.33±0.01	0.090±0.007	0.24±0.01
$CsPbBr_3@TiO_2$	1.56±0.02	0.24±0.01	0.038±0.0001	-	0.130±0.002
$CsPbBr_{1.95}I_{1.05}@TiO_2$	5.44±0.06	1.34±0.02	0.43±0.001	0.037±0.001	0.17±0.01
$CsPbBr_{1.65}I_{1.35}@TiO_2$	5.94±0.09	1.21±0.03	0.26±0.008	0.076±0.004	0.13±0.002

Figure 25. Photographs of $CsPbBr_3$ and $CsPbBr_3@TiO_2$ dispersed in a mixture of glycerol and water.

References

1 L. Protesescu, S. Yakunin, M. I. Bodnarchuk, F. Krieg, R. Caputo, C. H. Hendon, R. X. Yang, A. Walsh and M. V. Kovalenko, *Nano Lett.*, 2015, **15**, 3692–3696.

2 C. Lu, M. W. Wright, X. Ma, H. Li, D. S. Itanze, J. A. Carter, C. A. Hewitt, G. L. Donati, D. L. Carroll, P. M. Lundin and S. M. Geyer, *Chem. Mater.*, 2019, **31**, 62–67.

3 C. K. Møller, *Mat. Fys. Medd. Dan. Vid. Selsk.*, 1959, **32**, 1–18.

4 C. K. Møller, *The Structure of Perovskite-like caesium plumbo trihalides*, 1959, vol. 32.

5 A. Swarnkar, V. K. Ravi and A. Nag, *ACS Energy Lett.*, 2017, **2**, 1089–1098.